

Dynamic Dual-level Defense Routing for Continual Adversarial Training

Wenxuan Wang¹, Chenglei Wang¹, Xuelin Qian²

¹School of Computer Science, Northwestern Polytechnical University, National Engineering Laboratory for Integrated Aero-Space-Ground-Ocean Big Data Application Technology

²School of Automation, Northwestern Polytechnical University, the BRAin and Artificial INtelligence Lab
wxwang@nwpu.edu.cn, 1474515006wcl@gmail.com, xlqian@nwpu.edu.cn

Abstract

As adversarial attacks continue to evolve, defense models face the risk of recurrent vulnerabilities, underscoring the importance of continuous adversarial training (CAT). Existing CAT approaches typically balance decision boundaries by either data replay or optimization strategy to constrain shared model parameters. However, due to the diverse and aggressive nature of adversarial examples, these methods suffer from catastrophic forgetting of previous defense knowledge after continual learning. In this paper, we propose a novel framework, called Dual-level Defense Routing (DDeR), that can autonomously select appropriate routers to integrate specific defense experts, thereby adapting to evolving adversarial attacks. Concretely, the first-level defense routing comprises multiple defense experts and routers, with each router dynamically selecting and combining suitable experts to process attacked features. Routers are independently incremented as continuous adversarial training progresses, and their selections are guided by an Adversarial Sentinel Network (ASN) in the second-level defense routing. To compensate for the inability to test due to the independence of routers, we further present a Pseudo-task Substitution Training (PST) strategy, which leverages distributional discrepancy in data to facilitate inter-router communication without storing historical data. Extensive experiments demonstrate that DDeR achieves superior continuous defense performance and classification accuracy compared to existing methods.

Introduction

Deep neural networks have achieved remarkable success in various computer vision tasks, yet their vulnerability to adversarial attacks (Madry 2017) poses a significant challenge to their reliability and security. By introducing imperceptible perturbations to inputs, attackers can manipulate or induce the model to make incorrect predictions. To mitigate this risk, adversarial training has been proposed and developed as one of the most effective defense strategies. Adversarial training (Dong et al. 2023; Liu et al. 2025) strengthens model robustness by training with adversarial examples, enabling them to learn more resilient decision boundaries between benign and attack images.

Despite the effectiveness of adversarial training, the ongoing evolution of adversarial attacks presents a continu-

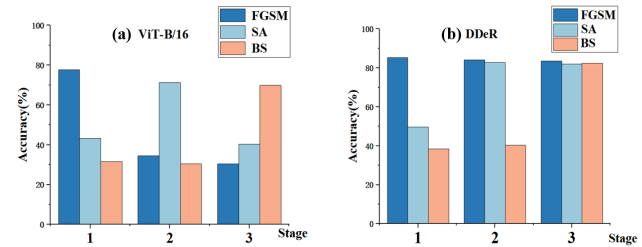


Figure 1: Perform continuous adversarial training (CAT) against attack sequence [FGSM (Goodfellow, Shlens, and Szegedy 2014), Square Attack (SA) (Andriushchenko et al. 2020), BruSLeAttack (BS) (Vo, Abbasnejad, and Ranasinghe 2024)]. At each training stage, we evaluate the robust accuracy of (a) baseline ViT-B/16 and (b) our method on the CIFAR-10 dataset against all attacks.

ous game of strategy between attackers and defenders. As new attack methods emerge, previously adversarially trained models may become vulnerable again, thus raising a critical question of ‘*whether the adversarial training can be continuously applied to counteract an ever-expanding range of adversarial attacks?*’ To answer this, we conduct a pilot study in Fig. 1(a). We find that while adversarial training initially improves the robustness of the model against current attacks, its defense against past attacks gradually weakens as training continues. This suggests that continuously applying adversarial training faces the well-known issue of catastrophic forgetting, which reveals the limitation of static or one-time adversarial training.

In this paper, we thus focus on the task of **Continual Adversarial Training (CAT)**, aiming to help models adapt to new adversarial attacks over time while maintaining their robustness. The challenge is to ensure that the model learns to defend against new attacks without forgetting previous defenses or causing knowledge conflicts. A straightforward approach is to apply methods from traditional continual learning (Wang et al. 2024a). For example, some works (Wang et al. 2024b, 2023) store previously used training data and replay it during training to retain defense knowledge. However, this raises privacy concerns. Other studies (Zhou and Hua 2024) use data augmentation and knowledge distillation to refine decision boundaries, but often lead to performance trade-offs. Moreover, all these approaches rely on a common

set of model parameters for all attack sequences. As a result, the model struggles to balance different defense strategies effectively, leading to suboptimal performance.

To this end, we propose a novel framework, called Dual-level Defense Routing (DDeR), for continual adversarial training. Draw inspiration from MoE (Mustafa et al. 2022), our first-level defense routing contains a set of defense experts and routers. The router can automatically select several appropriate experts to process the input, minimizing the negative effects of adversarial noise hidden in the image. This level highlights the significance of knowledge sharing. Although the set of experts is the same for all kinds of adversarial attacks, including past and potential future attacks, the robustness of models against diverse adversarial attacks can be effectively strengthened by integrating the knowledge of different experts. Our second-level defense routing is guided by an Adversarial Sentinel Network (ASN), a sub-network that operates independently of the main model. The role of ASN is to assign a suitable router to the incoming image. The number of routers is designed to grow gradually as continual adversarial training progresses. Such an incremental design of independent structures effectively mitigates the limitations of knowledge forgetting or conflict that arise in the parameter-sharing model, as shown in Fig. 1(b). Meanwhile, each router is instantiated by a fully connected layer, the increase in the number of parameters is thus minimal.

The purpose of ASN is not to recognize the specific category of adversarial perturbations, but to determine which router should process the input. However, since routers are trained independently and unaware of each other, and attack types are unknown at inference, the ASN remains disabled during inference. To address this, we further introduce a Pseudo-task Substitution Training (PST) strategy, which leverages the distribution discrepancy in image data to establish correlations between routers. More concretely, we first store the mean and covariance of each dataset used in continual adversarial training. Then, we use the re-parameterization technique (Wang et al. 2019) to sample training images and train ASN to classify which stage of continual adversarial training the input image belongs to. It can not only tackle the problem of ASN training/testing but also eliminate the need to store large amounts of historical training data, thereby avoiding privacy issues. Our contributions can be summarized as follows,

- We propose a Dynamic Dual-Level Defense Routing framework for Continual Adversarial Training, which autonomously selects appropriate routers to integrate knowledge from different specialized experts, ensuring effective feature representation and enhancing the model’s resilience against evolving adversarial attacks.
- We propose a Pseudo-task Substitution Training strategy to assist the Adversarial Sentinel Network in selecting an appropriate router for processing inputs. This strategy leverages the data distribution discrepancy to establish correlations between routers, reducing historical data storage requirements and mitigating privacy risks.
- Our method achieves the SOTA defense performance over multiple attack sequences among CIFAR-10,

CIFAR-100, and ImageNet-1K datasets, maintaining high accuracy on clean samples and unseen corruption attacks. This demonstrates its sustained robustness against evolving attack methods.

Related Work

Adversarial Attacks. Adversarial attacks (Li et al. 2025a, 2023) mislead deep learning models by adding subtle perturbations to the input. Based on the attacker’s access to model information, these attacks are categorized into white-box and black-box types. White-box attacks (Carlini and Wagner 2017; Xu, Zheng, and Guo 2025) assume full knowledge of the model’s architecture, parameters, and gradients, and typically generate perturbations using gradient-based, optimization-based, or decision-boundary-based methods. Though highly effective, their practicality is limited. In contrast, black-box attacks (Yang et al. 2024; Jia et al. 2022; Park, McLaughlin, and Alouani 2025; Ren et al. 2025) require no internal model knowledge and rely solely on input-output behavior, often leveraging adversarial transferability or query-based strategies. As attack techniques continue to evolve, developing robust and sustainable defense mechanisms has become an urgent priority.

Adversarial Training. Adversarial training (Madry 2017), which enhances model robustness by incorporating adversarial examples during training, has become a leading defense strategy. Recent approaches improve performance by introducing regularization (Li et al. 2025b), knowledge distillation (Levi et al. 2025), and loss-smoothing techniques (Wei, Guo, and Wang 2025). AUTE (Huang et al. 2025) combines ensemble models with peer-alignment and self-unlearning techniques to effectively enhance adversarial robustness during training. However, adversarial training often sacrifices standard accuracy, prompting research on balancing robustness and clean accuracy. For instance, soft labels and logit-based regularization frameworks (Yin and Ruan 2024) are developed to address this trade-off. Nonetheless, large domain gaps between adversarial samples and the issue of catastrophic forgetting in defense models continue to hinder adaptation to evolving attacks and the realization of sustained robustness.

Continuous Adversarial Defense. As attacks are iteratively updated, researchers begin to focus on how to achieve a defense mechanism that continuously expands the attack sequence through adversarial training. Recent studies propose various solutions from the perspective of memory replay. (Zhou and Hua 2024) proposes an Anisotropic and Isotropic Replay-based Lifelong Defense (AIR), which constructs pseudo-replay data through data augmentation to mitigate the model’s forgetting of past samples. However, given the wide variety of attack types, AIR, a data augmentation-based approach, may fail when there are significant differences between different types of samples. (Wang et al. 2024b) proposes a Sustainable Self-Evolving Adversarial Training (SSEAT), which involves setting up a buffer to store past samples and utilizing knowledge distillation to effectively balance the model’s accuracy on clean samples while defending against different adversarial samples. How-

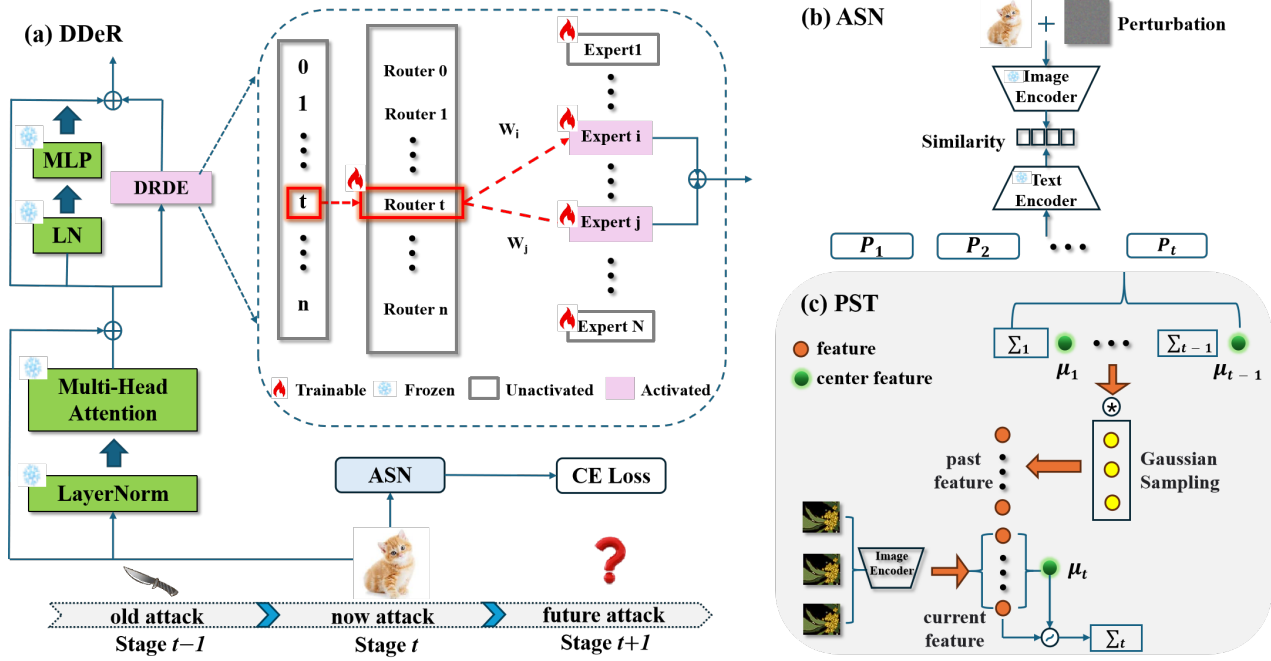


Figure 2: (a) Schematic diagram of DDeR. During training, each attack type is assigned to a dedicated router, which processes image features from the multi-head attention mechanism and generates expert weights to aggregate multiple expert outputs. (b) The training process of ASN. We represent textual information for each attack type using context vectors and class word embeddings, which are fed into a text encoder to compute similarity scores with input image features. The context vectors are then updated via cross-entropy loss. (c) Autonomous Router Selection via PST. We propose a feature-space-enhanced PST strategy that utilizes distributional variations in image data to establish correlations between routers, ensuring the accurate assignment of images to the appropriate router.

ever, these works have high data storage requirements and privacy issues.

Methodology

Task Definition and Framework Overview

Task Definition. To develop a defense algorithm adaptable to evolving attacks, we address the Continuous Adversarial Training (CAT) task. Analogous to task-incremental learning, the model sequentially learns a series of attacks $\mathcal{A} = \{A^0, A^1, \dots, A^t, \dots\}$, where A^t denotes the t_{th} type of attack and A^0 represents clean samples. At t_{th} stage, the training dataset $A^t = \{x_i^t, y_i^t\}_{i=1}^{N^t}$ comprises adversarial inputs x_i^t , their labels y_i^t , and dataset size N^t . The attack type t is provided during training to guide robustness learning, but is not available during inference, aligning with real-world deployment scenarios. Evaluation is performed on samples from all attack types.

Framework Overview. As shown in Fig. 2(a), we propose a Dynamic Dual-level Defense Routing (DDeR), a novel framework designed to enhance defense adaptability against evolving attack sequences through a dynamically scalable architecture, addressing the limitations of shared model parameters. Our first-layer defense routing is inspired by MoE (Mustafa et al. 2022) and built upon a frozen CLIP model (Radford et al. 2021). It integrates a set of defense experts and a router to form Dynamic Routing of Defensive Experts (DRDE). The router autonomously

selects a combination of optimal experts, implemented as lightweight LoRA (Hu et al. 2021) modules, to process inputs, promoting efficient knowledge sharing and specialization. The second-level defense routing is managed by the Adversarial Sentinel Network (ASN), which operates independently to assign appropriate routers to incoming images. To ensure ASN remains effective during inference despite routers learning independently during training, we introduce Pseudo-task Substitution Training (PST), which exploits distributional discrepancies in image data to establish inter-router correlations.

Dynamic Routing of Defensive Experts

To cope with the continuous emergence of novel attack types and the problem of suboptimal defense performance caused by all samples sharing the same set of model parameters, we propose a Dynamic Routing of Defense Experts (DRDE) module, which is an extensible architecture based on MoE (Mustafa et al. 2022). DRDE continuously expands the router as new attack types increase, aggregating the outputs of defense experts for each attack type to form a specific result, thereby achieving adaptive and optimized defense strategies. For attack type t , DRDE contains a set of defense experts $\{M_i\}_{i=1}^n$ and a data-sensitive router \mathcal{R}^t , where n denotes the number of experts.

To ensure scalability and efficiency, we employ LoRA (Hu et al. 2021) as lightweight defense experts within DRDE, which decomposes frozen model parameters

into a low-rank trainable space, allowing efficient adaptation to diverse attacks with minimal computational overhead. Each router is implemented using a single fully connected layer, preventing an excessive increase in model parameters as the number of routers grows during continual adversarial training. This effectively mitigates issues such as knowledge forgetting and conflicts in parameter-sharing models.

Defensive Experts. In DRDE, the data-sensitive router \mathcal{R}^t dynamically selects and activates multiple defense experts $\{M_i\}_{i=1}^n$ to generate adaptive responses for each attack type t . The corresponding output $f(x_i^t)$ from experts is computed as:

$$f(x_i^t) = \sum_{i=1}^n W_i^t M_i(\mathbf{x}_i^t) \quad (1)$$

where $W^t = \{W_i^t\}_{i=1}^n$ indicates the gating weights assigned by \mathcal{R}^t , dictating each expert's contribution, and x_i^t represents the input image for attack type t .

Given the distinct data distributions of adversarial samples generated by different attack methods, the contribution of each expert should adapt dynamically to varying attack types. To achieve this, we incorporate image features \mathbf{f} into the router, enabling adaptive weight assignment to defense experts. The gating weights are computed as follows:

$$W^t = \text{Softmax}(\text{topk}(\mathcal{R}^t(\mathbf{f}))) \quad (2)$$

where \mathcal{R}^t projects image features \mathbf{f} onto a 1-D vector, quantifying each expert's contribution. The $\text{topk}(\cdot)$ selects the top k most influential experts by assigning their corresponding weights to them while setting $-\infty$ for the remaining experts. Finally, $\text{Softmax}(\cdot)$ is applied to normalize the selected weights, achieving optimal expert aggregation.

Dynamic Expert Updating. To adapt the model to emerging attacks, we introduce a Dynamic Expert Updating (DEU) strategy, which facilitates the addition of new routing modules and updates to defense expert parameters when a novel attack is encountered. Defense experts are trained via standard backpropagation, guided by a momentum-based fusion strategy to retain past knowledge and foster cross-type collaboration, thus mitigating catastrophic forgetting and enhancing robustness. Specifically, after training on previous data, the top k most active expert parameters are stored temporarily to maintain type-specific knowledge. When a new attack emerges, these stored parameters are linearly fused with the existing ones, replacing the original expert parameters. The linear fusion is defined as:

$$\psi^* = \rho\psi_v + (1 - \rho)\psi_u \quad (3)$$

where ψ^* denotes the fused expert parameters, ψ_v and ψ_u represent the temporarily stored expert parameters and the expert parameters from the trained model, respectively. The fusion weight ρ controls the balance between the old and new parameters, which is set to 0.5 to prioritize the retention of knowledge from previous attacks. This allows the router to access stored parameters when encountering new tasks, leveraging past knowledge while optimizing experts for task-specific features, thereby preserving and effectively utilizing historical information.

Adversarial Sentinel Network

In real-world scenarios, the attack type of a sample is unavailable during testing, so the sample cannot be assigned to the appropriate router. To enable autonomous assignment of the most suitable router for each input, we introduce an Adversarial Sentinel Network (ASN), which fully leverages CLIP's prompt learning capability to construct learnable textual vectors for each attack type. These vectors are fed into the text encoder to generate a set of text features. We then compute the similarity between these text features and the image features, which allows the system to automatically match the input to the most relevant router, enabling the router to integrate outputs from the corresponding experts and produce the final result.

Specifically, the textual vectors are composed of a class word vector and context vectors. The class word vector for the attack type t is defined as TYPE_t . Different from using fixed templates to generate context vectors directly from original text, we adopt a set of M learnable vectors $[V]_m$ (where $m \in 1, \dots, M$) to represent the context vectors of attack type t . These vectors are defined in the word embedding space, making them learnable and providing greater adaptability. Each vector has the same dimensionality as a word embedding, *i.e.*, 512. The final textual vectors P_t to the text encoder are the concatenation of the context vectors and the class word vector, as shown below:

$$P_t = [V]_1 \dots [V]_M [\text{TYPE}_t] \quad (4)$$

ASN learns distinct context vectors for each attack type, enabling customized context that facilitates accurate router assignment. We optimize the context parameters using cross-entropy loss. Subsequently, the similarity logits between image and text features are computed to guide router selection and integrate outputs accordingly.

Pseudo-task Substitution Training

During ASN training, each stage involves only one attack type, resulting in independent routers. However, at inference time, the attack type of a test sample is unknown, and this lack of inter-router coordination hampers accurate router selection, causing ASN failure. To address this, a router capable of adapting to unseen data is required. While data replay can revisit past knowledge to guide router selection in CAT, it incurs substantial storage overhead.

Recent studies (Wang et al. 2021, 2019) show that feature expansion in deep feature space can generate diverse intra-class representations, effectively augmenting data at the feature level. Inspired by this, we propose a Pseudo-task Substitution Training (PST) strategy to mitigate the storage cost of saving original samples. PST leverages the mean and covariance matrix of stored features from previous attack types to expand feature representations, allowing the ASN to incorporate prior data features during router training. This approach establishes correlations between routers while reducing storage requirements.

Specifically, as in Fig. 2(c), in the feature space, we compute the “center” of each attack type, *i.e.*, the average feature representation. Then, we calculate the variance between the

METHODS	FGSM	BIM	PGD	SA	BS	MCG	DIM	Clean
PGD-AT	48.92	47.08	50.58	45.32	42.83	40.65	47.12	72.13
AWP	44.50	41.89	48.12	40.93	41.36	43.82	40.21	68.77
RIFT	51.65	52.91	53.89	49.21	51.72	50.45	47.91	73.54
LBGAT	53.14	53.22	54.37	51.26	52.89	52.33	50.10	71.95
AFD	51.12	51.45	53.14	50.83	50.65	52.78	49.56	72.41
SSEAT	54.82	55.47	56.47	56.11	57.65	56.37	55.93	71.52
DDeR (<i>Ours</i>)	60.71	61.23	62.83	61.55	63.07	62.47	64.14	75.92

Table 1: Comparison results under a long attack sequence [FGSM, BIM, PGD, SA, BS, MCG, DIM] on ImageNet-1K.

center and feature representations of samples with the same attack type within each mini-batch. These variances are progressively aggregated into a covariance vector using a moving average, which can be formulated as:

$$\Sigma_t = \mathbb{E}[(\mu_t - f_t)^2] \quad (5)$$

Resampling the feature representations of past attack types based on the covariance matrix and mean can be defined as:

$$f_k = \mu_k + L_k z \quad (6)$$

$$\Sigma_k = L_k L_k^T \quad (7)$$

where f_k is the sampled feature from the past attack type k . z is a random vector sampled from a standard normal distribution $\mathcal{N}(0, I)$. L_k is the Cholesky decomposition matrix of the covariance matrix Σ_k . In training new attacks, we sample features from the stored mean and covariance matrices of past attack types to generate a subset of features. This process enriches the diversity of features and helps form correlations between routers to achieve input-based router adaptive selection during the inference phase.

Experimental

Experimental Setting

Datasets. We evaluate our method on ImageNet-1k (Deng et al. 2009), which is a widely used benchmark in adversarial attack and defense research. The model sequentially encounters a series of attacks, with training and testing data generated according to the corresponding attack methods. The model is trained on the generated adversarial examples over the training set, while the test set is exclusively used to assess its robustness. *More experimental results over CIFAR-10 and CIFAR-100 (Krizhevsky, Hinton et al. 2009) can be found in the Supplementary Material.*

Attack Algorithms. We assess the robustness of all baselines on ImageNet-1k against various strong adversarial attacks. (1) For Fast Gradient Sign Method (FGSM) (Goodfellow, Shlens, and Szegedy 2014) with perturbation size $\epsilon = 8/255$. For Projected Gradient Descent (PGD) (Madry 2017) with $\epsilon = 8/255$, step size as $2/255$, and the steps as 20. For CW attack (Carlini and Wagner 2017) with steps as 1000 and learning rate as 0.01. For DIM (Wu et al. 2021) with $\epsilon = 16/255$ 16/255, steps as 10, and weight parameters as 1.0. For DeepFool (Df) (Moosavi-Dezfooli, Fawzi, and Frossard 2016) with steps as 50 and an overshoot of 0.02. For AutoAttack (AA) (Croce and Hein 2020) with ϵ

as 8/255. For Square Attack (SA) (Andriushchenko et al. 2020) with the number of queries as 10,000 and $\epsilon = 0.05$. For BruSLeAttack (BS) (Vo, Abbasnejad, and Ranasinghe 2024) with the queries as 1000 and the sparsity as 0.2%. For MCG (Yin et al. 2022) with the number of queries as 10,000 and $\epsilon = 0.0325$. (2) For the unseen adversaries, we follow the implementation of (Jiang and Singh 2024), setting $\epsilon = 12$ for the fog attack, $\epsilon = 0.5$ for the snow attack, $\epsilon = 60$ for the Gabor attack, $\epsilon = 0.125$ for the elastic attack, and $\epsilon = 0.125$ for the jpeglf1nf attack with 100 iterations. (3) For attacks with different norms, similar to (Croce and Hein 2022), we use APGD with 5 steps for l_∞ and l_2 attacks and 15 steps for l_1 attacks. The perturbation budgets are set to $\epsilon_1 = 12, \epsilon_2 = 0.5, \epsilon_\infty = 8/255$.

Implementation Details. We conduct experiments on a single NVIDIA RTX 3090 GPU with PyTorch. For ImageNet-1K, images are resized to 224×224 and augmented using horizontal flipping and random cropping. The model architecture is ViT-B/16. For training, we use a batch size of 64 and optimize the model using the Adam optimizer with a learning rate of 1×10^{-3} . The router and expert parameters are trained for 30 epochs. During ASN training, a context vector of length 16 was learned over 20 epochs.

Competitors. We compare with traditional adversarial training, such as PGD-AT (Madry 2017), AWP (Wu, Xia, and Wang 2020), RIFT (Zhu and X. 2023), LBGAT (Cui et al. 2021) and AFD (Zhou et al. 2025). Meanwhile, we compare with CAT method SSEAT (Wang et al. 2024b) under the same settings. For fairness, traditional adversarial training methods are further fine-tuned on adversarial attacks, with knowledge distillation (Hinton, Vinyals, and Dean 2014) applied between old and updated models to mitigate catastrophic forgetting. All competitors use the ViT-B/16 model.

Evaluation Metrics. We set different attack sequences, including [FGSM, PGD, CW, AA, Df], [FGSM, BIM, PGD, SA, BS, MCG, DIM], and [L_∞, L_2, L_1]. After CAT models undergo continual training following the attack sequence and the traditional adversarial training methods complete their respective training processes, we evaluate their robustness against all attacks in the sequence, as well as their classification accuracy on clean test data.

Experimental Results

We evaluate the defense performance of DDeR against various competitors on several datasets, assessing its robustness across diverse attack methods, adversarial perturbations

METHODS	FGSM	PGD	CW	AA	Df	Clean
PGD-AT	46.71	37.44	38.08	37.66	38.97	60.12
AWP	49.85	40.21	41.12	40.46	40.38	64.91
RIFT	51.82	47.37	46.31	46.22	48.09	62.55
LBGAT	48.76	44.59	45.07	44.38	45.66	61.73
AFD	52.03	53.11	53.89	53.27	54.42	66.18
SSEAT	56.84	57.36	58.75	59.41	59.07	61.01
DDeR (<i>Ours</i>)	68.56	67.38	68.53	68.49	69.79	70.34

Table 2: Comparison results under a short attack sequence [FGSM, PGD, CW, AA, Df] on the ImageNet-1K.

METHODS	L_∞	L_2	L_1	UNION	CLEAN
PGD-AT	51.83	36.11	29.29	29.29	74.12
AWP	48.24	36.40	28.05	28.05	71.12
LBGAT	52.97	38.02	31.41	31.41	72.83
RIFT	56.41	40.52	34.21	34.21	74.03
AFD	54.09	39.70	33.75	33.75	73.51
SSEAT	56.80	41.19	36.94	36.94	73.89
DDeR (<i>Ours</i>)	58.33	42.75	38.21	38.21	76.84

Table 3: Comparison results against adversarial attacks with different norms under the CAT task on ImageNet-1K.

under different norms, and clean samples. Additionally, we compare the number of learnable parameters and peak memory allocation of ours and competitors. **DDeR effectively realizes the best defense performance against several attack sequences and achieves the highest accuracy over clean samples.** As in Tab. 1 and Tab. 2, under various attack sequences, our DDeR bests all competitors with large margins over both clean and adversarial samples. Besides, we evaluate robustness under attack sequences that differ in perturbation norms as shown in Tab. 3. Consistent with prior findings (Tramer and Boneh 2019), our results confirm that improving robustness to one perturbation may inadvertently increase susceptibility to others. Nevertheless, DDeR achieves the highest union accuracy (Laidlaw, Singla, and Feizi 2020) among all methods, demonstrating superior general robustness. The above results demonstrate the superiority of DDeR on CAT task, which stems from its optimized selection and combination of expert knowledge, enabling more precise decision boundaries for different inputs.

DDeR achieves superior defense against unseen attacks. Trained on attack sequence [FGSM, PGD, CW, AA, Df] using ImageNet-1K, DDeR is evaluated on unseen natural corruptions (Jiang and Singh 2024). In Tab. 4, DDeR outperforms all competitors across all unseen attacks. This demonstrates its ability to generalize by leveraging knowledge from known attacks for effective router selection and prediction. Additionally, DDeR achieves a superior robustness-accuracy tradeoff, highlighting its universal robustness.

DDeR exhibits lower memory consumption and requires fewer learnable parameters than competitors for the CAT task. As in Tab. 5, our DDeR requires significantly less memory than rehearsal-based models, which incur ad-

METHODS	fog	snow	gabor	elastic	jpeglf1n
PGD-AT	40.24	21.37	41.87	48.14	48.56
AWP	35.78	22.34	39.20	42.89	45.37
RIFT	44.59	32.59	47.37	57.37	53.46
LBGAT	42.15	30.28	44.73	54.18	50.22
AFD	45.36	39.25	48.67	50.66	55.48
SSEAT	44.13	35.79	49.17	51.32	58.72
DDeR (<i>Ours</i>)	47.49	48.31	53.49	60.45	59.36

Table 4: Comparison results about CAT models against unseen natural corruption attacks over ImageNet-1K.

METHODS	PM (MB)	Param	Cost (GFLOPS)
PGD-AT	22,543	82M	38.63
AWP	28,449	85M	45.17
LBGAT	25,475	92M	48.39
RIFT	28,173	103M	41.70
AFD	27,801	89M	42.58
SSEAT	32,475	83M	40.37
DDeR (<i>Ours</i>)	19,437	58K	23.78

Table 5: Comparison over Train-time peak memory allocation (PM), the number of learnable parameters (Param), and the total computational cost (Cost) on ImageNet-1K.

ditional storage overhead by retaining past samples. In contrast, DDeR dynamically expands a minimal number of parameters during training, storing only essential feature information and a limited set of historical parameters, thereby optimizing memory efficiency and making it more practical.

Ablation Study

To verify the role of each module in DDeR, we conduct extensive ablation studies on the following variants: (a) “Baseline”: conducted on CAT pipeline using the ViT-B/16 model; (b) “+DRDE”: building upon (a), we introduce shared experts and routers across all attack scenarios, along with a momentum-based parameter fusion strategy that incorporates historical parameters to guide the update of current model parameters; (c) “+DRDE+PST”: build upon (b), resampling features via using the mean and covariance matrix of feature representations from past samples; (d) “+DRDE+ASN”: build upon (b), we incorporate an Adversarial Sentinel Network (ASN) that exploits data distribution differences to improve router assignment. ASN trains context vectors using current-stage data to measure text-image feature similarity, producing logits that guide router selection; (e) “+DRDE+PST+ASN (Ours)”: build upon (d), to enhance the training data of ASN, we employ PST to sample historical examples, thereby improving data diversity.

The efficacy of each component in the proposed method. As shown in Tab. 6, by comparing the results of different variants, we notice the following observations, 1) According to the results of (a), based on the basic continual learning pipeline, the “Baseline” suffers from severe knowledge forgetting and fails to retain defense performance against prior

No.	Components			Method					
	DRDE	PST	ASN	FGSM	PGD	CW	AA	Df	Clean
<i>a</i>	×	×	×	48.22	49.73	46.46	50.38	58.13	49.33
<i>b</i>	✓	×	×	54.17	55.93	55.26	56.39	62.32	54.46
<i>c</i>	✓	✓	×	56.67	57.36	56.43	57.22	63.79	56.17
<i>d</i>	✓	×	✓	63.91	64.63	65.68	65.47	67.73	66.46
<i>e</i>	✓	✓	✓	68.56	67.38	68.53	68.49	69.79	70.34

Table 6: The ablation studies results of our proposed components in DDeR on ImageNet-1K.

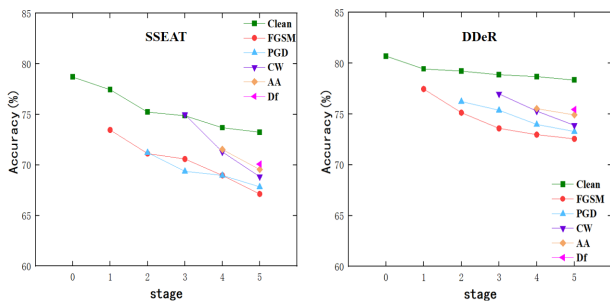


Figure 3: The accuracy of SSEAT and DDeR on both current and past attack data at each stage across the attack sequence [FGSM, PGD, CW, AA, Df] on ImageNet-1k.

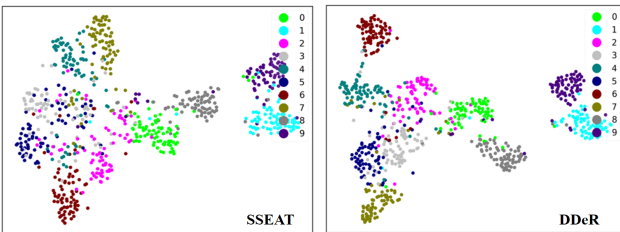


Figure 4: Visualizations of feature representations of clean samples by SSEAT and DDeR on ImageNet-1K. Different colors represent clean data of different categories. Zoom in for better views.

attacks; 2) Comparison between (a) and (b): Results show that introducing experts and routers yields modest performance gains across adversarial samples but does not effectively mitigate catastrophic forgetting; 3) Comparison between (b) and (c): Results indicate that PST effectively resamples critical past feature information, aiding the retention of previously learned robust representations; 4) Comparison between (b) and (d): Results demonstrate that using multiple routers with expert assignment per sample type mitigates shared parameter suboptimality, enhancing overall performance; 5) Comparison between (d) and (e): The results show that our model enhances ASN’s routing for inputs by storing only the mean and covariance of each dataset in CAT tasks, significantly reducing storage. Additionally, preserving representative features of each data type also leads to optimal performance.

METHODS	PGD _S ⁵⁰	PGD _S ²⁰	PGD _W ⁵⁰	PGD _W ²⁰	Clean
PGD-AT	22.71	25.84	47.95	52.31	60.42
AWP	19.34	23.06	42.88	47.12	57.89
RIFT	21.86	24.57	46.33	50.84	60.11
LBGAT	22.05	25.14	47.08	51.25	59.78
AFD	19.22	22.39	44.75	48.92	58.64
SSEAT	21.76	26.10	45.88	49.53	56.71
DDeR (<i>Ours</i>)	24.12	27.66	51.03	55.78	62.30

Table 7: Defense results with various attack strengths on ImageNet-1K. The *S* in the lower right corner indicates the strong attack perturbation size as 16/255, and the *W* indicates the weak attack perturbation size as 8/255.

Evaluation under increased attack intensity and iterations. Following the model setup in AIR (Zhou and Hua 2024), the forgetting phenomenon is more severe when progressing “from difficult to easy” tasks. To evaluate model robustness under varying difficulties, we gradually reduce the perturbation magnitude and the number of attack iterations. The CAT model is trained on a sequence of attacks: [PGD_S⁵⁰, PGD_S²⁰, PGD_W⁵⁰, PGD_W²⁰]. As shown in Tab. 7, DDeR consistently outperforms all competitors across all attack settings, achieving robust performance while maintaining high clean accuracy.

Visualization results. 1) As in Fig. 3, it shows the accuracy trajectories of SSEAT and DDeR on various adversarial attacks and clean samples during continual training. The results clearly demonstrate that DDeR achieves superior continual robustness and more effectively alleviates catastrophic forgetting. 2) As in Fig. 4, after training on [FGSM, PGD, CW, AA, Df], we randomly sampled 100 clean test images from 10 ImageNet-1K classes and extracted features via SSEAT and DDeR. t-SNE visualizations show that DDeR produces more discriminative features, with greater inter-class separation and tighter intra-class clustering, reflecting its strong clean-data accuracy.

Conclusion

We introduce DDeR for the CAT task, leveraging a corresponding router to adaptively select and integrate suitable experts based on input images, thereby enhancing continual adversarial robustness. To enable efficient router selection, we design the ASN module with PST strategy, leveraging distributional variations in image data to establish cor-

relations between routers, to accurately assign images to the appropriate router. Extensive experiments demonstrate that DDeR achieves state-of-the-art continual robustness and classification accuracy of benign images.

References

Andriushchenko, M.; Croce, F.; Flammarion, N.; and Hein, M. 2020. Square attack: a query-efficient black-box adversarial attack via random search. In *European conference on computer vision*, 484–501. Springer.

Carlini, N.; and Wagner, D. 2017. Towards evaluating the robustness of neural networks. In *2017 ieee symposium on security and privacy (sp)*, 39–57. Ieee.

Croce, F.; and Hein, M. 2020. Reliable evaluation of adversarial robustness with an ensemble of diverse parameter-free attacks. In *International conference on machine learning*, 2206–2216. PMLR.

Croce, F.; and Hein, M. 2022. Adversarial Robustness against Multiple and Single l_p -Threat Models via Quick Fine-Tuning of Robust Classifiers. In *International Conference on Machine Learning*, 4436–4454.

Cui, J.; Liu, S.; Wang, L.; and Jia, J. 2021. Learnable boundary guided adversarial training. In *Proceedings of the IEEE/CVF international conference on computer vision*, 15721–15730.

Deng, J.; Dong, W.; Socher, R.; Li, L.-J.; Li, K.; and Fei-Fei, L. 2009. Imagenet: A large-scale hierarchical image database. In *2009 IEEE conference on computer vision and pattern recognition*, 248–255. Ieee.

Dong, J.; Moosavi-Dezfooli, S.-M.; Lai, J.; and Xie, X. 2023. The enemy of my enemy is my friend: Exploring inverse adversaries for improving adversarial training. In *Proceedings of the IEEE/CVF Conference on Computer Vision and Pattern Recognition*, 24678–24687.

Goodfellow, I. J.; Shlens, J.; and Szegedy, C. 2014. Explaining and harnessing adversarial examples. *arXiv preprint arXiv:1412.6572*.

Hinton, G.; Vinyals, O.; and Dean, J. 2014. Distilling the knowledge in a neural network. In *NIPS Deep Learning and Representation Learning Workshop*. Presented at the Deep Learning and Representation Learning Workshop, NIPS 2014.

Hu, E. J.; Shen, Y.; Wallis, P.; Allen-Zhu, Z.; Li, Y.; Wang, S.; Wang, L.; and Chen, W. 2021. Lora: Low-rank adaptation of large language models. *arXiv preprint arXiv:2106.09685*.

Huang, L.; Su, T.; Gao, C.; Liu, N.; and Huang, Q. 2025. AUTE: Peer-Alignment and Self-Unlearning Boost Adversarial Robustness for Training Ensemble Models. In *Proceedings of the AAAI Conference on Artificial Intelligence*, volume 39, 3671–3679.

Jia, S.; Yin, B.; Yao, T.; Ding, S.; Shen, C.; Yang, X.; and Ma, C. 2022. Adv-attribute: Inconspicuous and transferable adversarial attack on face recognition. *Advances in Neural Information Processing Systems*, 35: 34136–34147.

Jiang, E.; and Singh, G. 2024. RAMP: Boosting Adversarial Robustness Against Multiple l_p Perturbations for Universal Robustness. *Advances in neural information processing systems*.

Krizhevsky, A.; Hinton, G.; et al. 2009. Learning multiple layers of features from tiny images.

Laidlaw, C.; Singla, S.; and Feizi, S. 2020. Perceptual adversarial robustness: Defense against unseen threat models. *arXiv preprint arXiv:2006.12655*.

Levi, Y. Y.; Grolman, E.; Yankelev, I.; Giloni, A.; Hofman, O.; Shimizu, T.; Shabtai, A.; and Elovici, Y. 2025. KDAT: Inherent Adversarial Robustness via Knowledge Distillation with Adversarial Tuning for Object Detection Models. In *Proceedings of the AAAI Conference on Artificial Intelligence*, volume 39, 4598–4606.

Li, S.; He, C.; Ma, X.; Zhu, B. B.; Wang, S.; Hu, H.; Zhang, D.; and Yu, L. 2025a. Enhancing Adversarial Transferability with Checkpoints of a Single Model’s Training. In *Proceedings of the Computer Vision and Pattern Recognition Conference*, 20685–20694.

Li, X.; Zhu, Y.; Huang, Y.; Zhang, W.; He, Y.; Shi, J.; and Hu, X. 2025b. PBCAT: Patch-based composite adversarial training against physically realizable attacks on object detection. In *ICCV*.

Li, Z.; Yin, B.; Yao, T.; Guo, J.; Ding, S.; Chen, S.; and Liu, C. 2023. Sibling-attack: Rethinking transferable adversarial attacks against face recognition. In *Proceedings of the IEEE/CVF conference on computer vision and pattern recognition*, 24626–24637.

Liu, X.; Yang, Y.; He, K.; and Hopcroft, J. E. 2025. Parameter Interpolation Adversarial Training for Robust Image Classification. *IEEE Transactions on Information Forensics and Security*.

Madry, A. 2017. Towards deep learning models resistant to adversarial attacks. *arXiv preprint arXiv:1706.06083*.

Moosavi-Dezfooli, S.-M.; Fawzi, A.; and Frossard, P. 2016. Deepfool: a simple and accurate method to fool deep neural networks. In *Proceedings of the IEEE conference on computer vision and pattern recognition*, 2574–2582.

Mustafa, B.; Riquelme, C.; Puigcerver, J.; Jenatton, R.; and Houlsby, N. 2022. Multimodal contrastive learning with limoe: the language-image mixture of experts. *Advances in Neural Information Processing Systems*, 35: 9564–9576.

Park, J.; McLaughlin, N.; and Alouani, I. 2025. Mind the Gap: Detecting Black-box Adversarial Attacks in the Making through Query Update Analysis. In *Proceedings of the Computer Vision and Pattern Recognition Conference*, 10235–10243.

Radford, A.; Kim, J. W.; Hallacy, C.; Ramesh, A.; Goh, G.; Agarwal, S.; Sastry, G.; Askell, A.; Mishkin, P.; Clark, J.; et al. 2021. Learning transferable visual models from natural language supervision. In *International conference on machine learning*, 8748–8763. PMLR.

Ren, Y.; Zhao, Z.; Lin, C.; Yang, B.; Zhou, L.; Liu, Z.; and Shen, C. 2025. Improving adversarial transferability on vision transformers via forward propagation refinement. In *Proceedings of the Computer Vision and Pattern Recognition Conference*, 25071–25080.

Tramer, F.; and Boneh, D. 2019. Adversarial training and robustness for multiple perturbations. *Advances in neural information processing systems*, 32.

Vo, V. Q.; Abbasnejad, E.; and Ranasinghe, D. C. 2024. Brusleattack: A query-efficient score-based black-box sparse adversarial attack. *arXiv preprint arXiv:2404.05311*.

Wang, L.; Zhang, X.; Su, H.; and Zhu, J. 2024a. A comprehensive survey of continual learning: Theory, method and application. *IEEE Transactions on Pattern Analysis and Machine Intelligence*.

Wang, Q.; Liu, Y.; Ling, H.; Li, Y.; Liu, Q.; Li, P.; Chen, J.; Yuille, A.; and Yu, N. 2023. Continual adversarial defense. *arXiv preprint arXiv:2312.09481*.

Wang, W.; Wang, C.; Qi, H.; Ye, M.; Qian, X.; Wang, P.; and Zhang, Y. 2024b. Sustainable Self-evolution Adversarial Training. In *Proceedings of the 32nd ACM International Conference on Multimedia*, 9799–9808.

Wang, Y.; Huang, G.; Song, S.; Pan, X.; Xia, Y.; and Wu, C. 2021. Regularizing deep networks with semantic data augmentation. *IEEE Transactions on Pattern Analysis and Machine Intelligence*, 44(7): 3733–3748.

Wang, Y.; Pan, X.; Song, S.; Zhang, H.; Huang, G.; and Wu, C. 2019. Implicit semantic data augmentation for deep networks. *Advances in Neural Information Processing Systems*, 32.

Wei, Z.; Guo, Y.; and Wang, Y. 2025. Identifying and Understanding Cross-Class Features in Adversarial Training. In *ICML*.

Wu, D.; Xia, S.-T.; and Wang, Y. 2020. Adversarial weight perturbation helps robust generalization. *Advances in neural information processing systems*, 33: 2958–2969.

Wu, W.; Su, Y.; Lyu, M. R.; and King, I. 2021. Improving the transferability of adversarial samples with adversarial transformations. In *Proceedings of the IEEE/CVF conference on computer vision and pattern recognition*, 9024–9033.

Xu, C.; Zheng, F.; and Guo, G. 2025. Stealthy False Data Injection Attacks in Multi-Channel Vehicular Communication: White-Box and Gray-Box Strategies. *IEEE Transactions on Vehicular Technology*.

Yang, Y.; Gao, R.; Wang, X.; Ho, T.-Y.; Xu, N.; and Xu, Q. 2024. Mma-diffusion: Multimodal attack on diffusion models. In *Proceedings of the IEEE/CVF Conference on Computer Vision and Pattern Recognition*, 7737–7746.

Yin, F.; Zhang, Y.; Wu, B.; Feng, Y.; Zhang, J.; Fan, Y.; and Yang, Y. 2022. Generalizable Black-box Adversarial Attack with Meta Learning. *IEEE transactions on pattern analysis and machine intelligence*.

Yin, X.; and Ruan, W. 2024. Boosting Adversarial Training via Fisher-Rao Norm-based Regularization. In *Proceedings of the IEEE/CVF Conference on Computer Vision and Pattern Recognition*, 24544–24553.

Zhou, N.; Zhou, D.; Liu, D.; Wang, N.; and Gao, X. 2025. Mitigating feature gap for adversarial robustness by feature disentanglement. In *Proceedings of the AAAI Conference on Artificial Intelligence*, volume 39, 10825–10833.

Zhou, Y.; and Hua, Z. 2024. Defense without Forgetting: Continual Adversarial Defense with Anisotropic & Isotropic Pseudo Replay. In *Proceedings of the IEEE/CVF Conference on Computer Vision and Pattern Recognition*, 24263–24272.

Zhu, H., K.; and X. 2023. Improving generalization of adversarial training via robust critical fine-tuning. In *CVPR*, 4424–4434.

Reproducibility Checklist

1. General Paper Structure

- 1.1. Includes a conceptual outline and/or pseudocode description of AI methods introduced (yes/partial/no/NA) **yes**
- 1.2. Clearly delineates statements that are opinions, hypothesis, and speculation from objective facts and results (yes/no) **yes**
- 1.3. Provides well-marked pedagogical references for less-familiar readers to gain background necessary to replicate the paper (yes/no) **yes**

2. Theoretical Contributions

- 2.1. Does this paper make theoretical contributions? (yes/no) **yes**
If yes, please address the following points:
- 2.2. All assumptions and restrictions are stated clearly and formally (yes/partial/no) **yes**
- 2.3. All novel claims are stated formally (e.g., in theorem statements) (yes/partial/no) **yes**
- 2.4. Proofs of all novel claims are included (yes/partial/no) **yes**
- 2.5. Proof sketches or intuitions are given for complex and/or novel results (yes/partial/no) **yes**
- 2.6. Appropriate citations to theoretical tools used are given (yes/partial/no) **yes**
- 2.7. All theoretical claims are demonstrated empirically to hold (yes/partial/no/NA) **yes**
- 2.8. All experimental code used to eliminate or disprove claims is included (yes/no/NA) **NA**

3. Dataset Usage

- 3.1. Does this paper rely on one or more datasets? (yes/no) **yes**
If yes, please address the following points:
- 3.2. A motivation is given for why the experiments are conducted on the selected datasets (yes/partial/no/NA) **yes**
- 3.3. All novel datasets introduced in this paper are included in a data appendix (yes/partial/no/NA) **NA**
- 3.4. All novel datasets introduced in this paper will be made publicly available upon publication of the paper with a license that allows free usage for research purposes (yes/partial/no/NA) **NA**
- 3.5. All datasets drawn from the existing literature (po-

tentially including authors' own previously published work) are accompanied by appropriate citations (yes/no/NA) **yes**

- 3.6. All datasets drawn from the existing literature (potentially including authors' own previously published work) are publicly available (yes/partial/no/NA) **yes**
- 3.7. All datasets that are not publicly available are described in detail, with explanation why publicly available alternatives are not scientificallyatisficing (yes/partial/no/NA) **yes**

4. Computational Experiments

- 4.1. Does this paper include computational experiments? (yes/no) **yes**
If yes, please address the following points:
- 4.2. This paper states the number and range of values tried per (hyper-) parameter during development of the paper, along with the criterion used for selecting the final parameter setting (yes/partial/no/NA) **partial**
- 4.3. Any code required for pre-processing data is included in the appendix (yes/partial/no) **partial**
- 4.4. All source code required for conducting and analyzing the experiments is included in a code appendix (yes/partial/no) **partial**
- 4.5. All source code required for conducting and analyzing the experiments will be made publicly available upon publication of the paper with a license that allows free usage for research purposes (yes/partial/no) **yes**
- 4.6. All source code implementing new methods have comments detailing the implementation, with references to the paper where each step comes from (yes/partial/no) **yes**
- 4.7. If an algorithm depends on randomness, then the method used for setting seeds is described in a way sufficient to allow replication of results (yes/partial/no/NA) **yes**
- 4.8. This paper specifies the computing infrastructure used for running experiments (hardware and software), including GPU/CPU models; amount of memory; operating system; names and versions of relevant software libraries and frameworks (yes/partial/no) **partial**
- 4.9. This paper formally describes evaluation metrics used and explains the motivation for choosing these metrics (yes/partial/no) **yes**
- 4.10. This paper states the number of algorithm runs used

to compute each reported result (yes/no) **yes**

4.11. Analysis of experiments goes beyond single-dimensional summaries of performance (e.g., average; median) to include measures of variation, confidence, or other distributional information (yes/no)
no

4.12. The significance of any improvement or decrease in performance is judged using appropriate statistical tests (e.g., Wilcoxon signed-rank) (yes/partial/no) **no**

4.13. This paper lists all final (hyper-)parameters used for each model/algorithm in the paper's experiments (yes/partial/no/NA) **yes**